International Journal of Innovative
Computing, Information and Control
Volume **9**, Number **6**, June **2013**

 ISSN 1349-4198
pp. **2597–2618**

OVERLAPPING DECOMPOSITIONS-BASED ROBUST DECENTRALIZED TABU SEARCH-OPTIMIZED FIXED STRUCTURE H_∞ FREQUENCY STABILIZER DESIGN IN INTERCONNECTED POWER SYSTEMS

Issarachai Ngamroo

School of Electrical Engineering
Faculty of Engineering
King Mongkut's Institute of Technology Ladkrabang
Bangkok 10520, Thailand
knissara@kmitl.ac.th

Received March 2012; revised July 2012

Abstract. *As interconnected power systems are subjected to load disturbances with changing frequency in the vicinity of the inter-area oscillation mode, the system frequency may severely oscillate. To stabilize frequency oscillation, the dynamic power flow control devices can be exploited. This paper focuses on a new robust decentralized fixed structure H_∞ frequency stabilizer design of power control devices based on overlapping decompositions. The tie-line between two interconnected systems can be treated as the overlapped variable so that the original system can be decomposed into two subsystems. The frequency stabilizer equipped with the power control device can be designed in each subsystem independently. The structure of frequency stabilizer is specified as the 2^{nd} -order lead/lag compensator. To augment the system robust stability, the multiplicative uncertainty is employed to represent all unstructured system uncertainties. As a result, the multiplicative stability margin (MSM) can be used to guarantee the system robust stability. The control parameters of frequency stabilizer are optimized by a tabu search, so that the desired damping ratio of the target inter-area mode and the highest MSM are achieved. Two examples of power flow devices, i.e., high-voltage direct current transmission system and superconducting magnetic energy storage, are used to show the high performance and robustness against load disturbances and system parameters variation.*
Keywords: Overlapping decompositions, H_∞ control, Tabu search, Robust stability, System uncertainties, Frequency stabilization

1. **Introduction.** Currently, an increase in electric energy consumptions as well as regulatory constraints, has forced power companies to operate the power systems near stability limits. To handle this situation, the interconnections among power systems have been extensively performed so that the system security, economics and flexibility of system operation can be achieved [1]. Nevertheless, when the large load change suddenly occurs in a power system, the system frequency may be considerably perturbed from the normal value. Especially, if the frequency of changing load is in the vicinity of the inter-area mode (0.2-0.8Hz), the system frequency oscillation may experience a serious stability problem [2]. In the worst scenario of the undamped frequency oscillation, the power system may be unstable. Consequently, the cascade tripping, the partial or complete blackout will occur eventually.

Under this situation, the conventional frequency control, i.e., a governor, may no longer be able to compensate for such load changes due to its slow response. Furthermore, since a governor has no any stabilizing effect on the inter-area mode, the stabilization of frequency oscillation cannot be expected [3]. To eliminate the frequency oscillation, several power

system controllers equipped with the synchronous generators have been applied in the past. In [4], the wide area power system stabilizer (PSS) based on support vector machine has been presented. Besides, the robust automatic voltage regulator (AVR) design based on mixed H_2/H_∞ pole placement using linear matrix inequality has been proposed in [5]. Nevertheless, it has been proved in [6-8] that the stabilizing effect of power system controllers such as PSS and AVR is inferior to that of the dynamic power flow control devices.

Among of dynamic power flow control devices, High-Voltage Direct Current (HVDC) transmission system and Superconducting Magnetic Energy Storage (SMES) have been expected as the sophisticated series and shunt devices, respectively. First for the HVDC link, it offers major advantages such as a long distance power transmission, an enhancement of system damping etc., [9]. In addition, the HVDC link can be applied as an energy transfer device from a power system to compensate for rapid load changes in another system. As a result, the HVDC link can be applied to overcome the frequency oscillation problem. Several design methods of frequency stabilizer of HVDC link have been proposed, such as a linear optimal regulator [10], a fuzzy control [11] etc. However, the structure of these proposed controllers is not easy to implement in practical systems. Besides, these design methods have not taken system uncertainties due to variations of system parameters into consideration, and the robustness of resulted frequency stabilizer against uncertainties cannot be guaranteed.

For the SMES, it is expected as the advanced power control device since it is capable of controlling active and reactive power simultaneously [12]. Accordingly, an SMES can be applied to frequency stabilization. Several frequency stabilizer designs of SMES have been proposed such as an adaptive control [13], a neural network [14] and a fuzzy control [15] etc. Nevertheless, the structure of these proposed controllers is impractical for actual power systems. In addition, the robustness cannot be guaranteed in the face of system uncertainties.

To enhance the robustness, the H_∞ control which is one of the most advanced robust control theories, has been paid attention in various studies [16]. Even if the H_∞ controllers proposed in recent literatures provide successfully control effect, the remaining problem is the high order of resulted controllers. To solve this problem, the H_∞ fixed-structure controller has been presented [17]. Nevertheless, the selection of weighting functions is still an inevitable problem for the H_∞ fixed-structure controllers in these works.

To achieve a robust controller with low order without difficulty of weighting functions selection, a new robust decentralized fixed structure H_∞ frequency stabilizers design based on overlapping decompositions is proposed in this paper. Treating the tie-line between two interconnected systems as the overlapped variable, two subsystems can be decomposed from the original system [18]. As a result, the frequency stabilizer can be independently designed in each subsystem. The 2^{nd}-order lead/lag compensator is used as the specified structure of frequency stabilizer. All possible unstructured system uncertainties are represented by the multiplicative uncertainty [19]. A tabu search (TS) [20] is applied to optimally tune the control parameters of frequency stabilizer, so that the desired damping ratio of the target inter-area mode and the best stability margin are achieved. Two examples of power flow control devices, i.e., HVDC and SMES, are used to demonstrate the effect of the proposed control design. The high performance and robustness of the proposed frequency stabilizer against load disturbances and system parameters variation are confirmed by simulation studies.

2. **Study System and Modeling.**

The three-area interconnected power systems shown in Figure 1 are used to explain the motivation of the proposed control design. It is assumed

that large loads with sudden change, such as large steel mills, arc-furnace factories, magnetic levitation transporters and testing plants for nuclear fusion etc., have been placed each area. The total active power absorbed by such loads exhibits a periodical variation with multiple frequencies of inter-area oscillation modes. This results in a serious problem of frequency oscillations in each area. Frequency oscillations will severely affect the production quality of frequency-sensitive industries such as spinning and weaving industry, petrochemical industry, making-paper industry and semiconductor industry. In addition, the life time of machine apparatuses on load side will be reduced. Furthermore, many independent power producers (IPPs) which have not sufficient abilities of frequency control, have been installed in each area. As a result, the ability of governor in each area to provide frequency control is not adequate. To stabilize frequency oscillation, two power flow control devices with series or parallel connection have been installed.

The motivation of the research work can be strengthened as follows.

1) Many of nowadays' technological and social problems involve very complex and large dimensional systems. For such systems, it is usually necessary to avoid centralized controllers due to a number of reasons such as the cost of implementation, complexity of on-line computations, complexity of controller design and reliability. In such a situation, a decentralized or overlapping feedback structure may be used. A particular overlapping feedback structure may be selected either due to certain design consideration such as geographical location, cost of information transfer and reliability, or simply to match the overlapping structure of the given system. The underlying idea in the latter case is the expectation that such a controller may perform better than both a non-overlapping (completely decentralized) controller and a centralized controller.

2) It is advantageous to recognize the fact that subsystems share common parts in a wide variety of natural and man-made stochastic systems, such as freeway traffic regulations [21], socioeconomic systems [22], electric power systems [23] and large space structure [24], so a logical way is to establish a decentralized control scheme by applying the overlapping decompositions.

3) From the practical point of view, power system utilities prefer a controller with simple structure which is easy to implement. To serve this requirement, the structure of the proposed controller is specified as the 2^{nd}-order lead-lag compensator. This practical structure not only provides the ease of online tuning, but also assures the stability and reliability of the controller. Moreover, the controller parameters can be automatically tuned by the proposed optimization technique.

4) Under the various uncertainties in power systems such as unpredictable load changes and system parameters variation etc., the proposed optimization can guarantee the designed controller which is very robust against system uncertainties.

The linearized state equation of the original system in Figure 1 for frequency stabilization study can be given by

$$S: \begin{bmatrix} \dot{x}_1 \\ \dot{x}_2 \\ \dot{x}_3 \end{bmatrix} = \begin{bmatrix} A_{11} & A_{12} & A_{13} \\ A_{21} & A_{22} & A_{23} \\ A_{31} & A_{32} & A_{33} \end{bmatrix} \begin{bmatrix} x_1 \\ x_2 \\ x_3 \end{bmatrix} + \begin{bmatrix} B_{11} & B_{12} \\ B_{21} & B_{22} \\ B_{31} & B_{32} \end{bmatrix} \begin{bmatrix} u_1 \\ u_2 \end{bmatrix} \tag{1}$$

where x_i is state variable, u_i is control input from the frequency stabilizers, A_{ij} is the sub-matrix of the system matrix, B_{ij} is the sub-matrix of input matrix. The sub-matrices A_{ij} and B_{ij}, $(i, j = 1, 2, 3)$ have appropriate dimensions identical to the corresponding states and input vectors. This system is referred to as system "S".

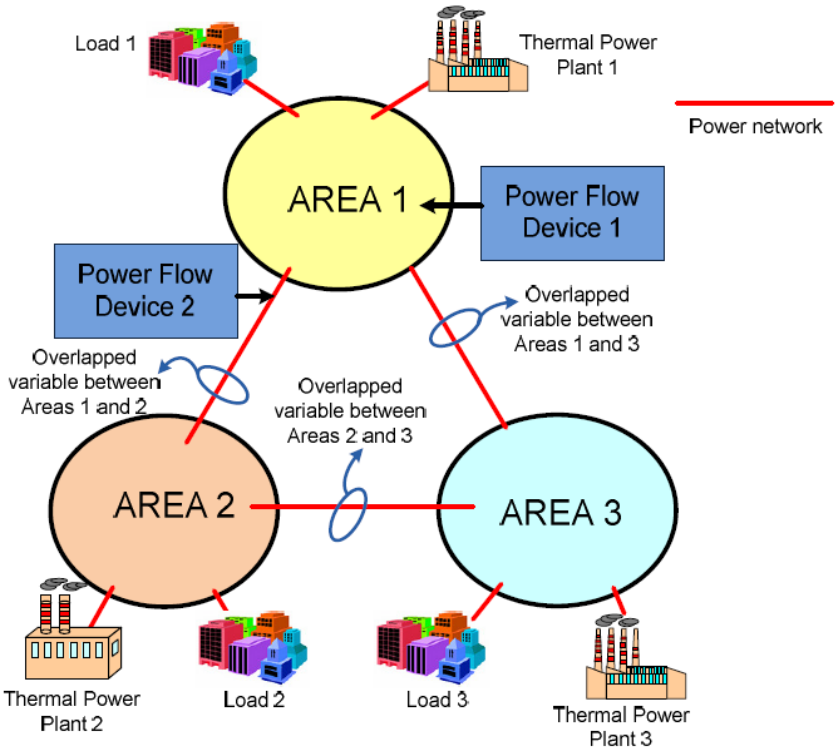

FIGURE 1. Multi-area interconnected power systems with power flow devices

3. **Proposed Control Design.**

3.1. **Overlapping decompositions.** In the topic of large scale and complex systems such as mechanical systems, electric power systems and vehicles etc., it is frequent to work with systems with share some components. This kind of systems can be treated as interconnected systems with overlapped subsystems (The subsystems share common parts). The overlapping decompositions of a large scale system allow the subsystems to share some common parts and thus provide greater flexibility in the choice of the subsystems [25]. The theory behind the overlapping decompositions is Inclusion Principle [26], which justifies the embedding of a finite dimensional system into a higher dimensional system. The overlapping decompositions of the original system correspond to a disjoint decomposition of the expanded system. A decentralized solution for the (disjoint) pieces of the expanded system is then contracted to obtain a solution for the original system.

The concept of overlapping decompositions has been successfully applied to various large-scale problems including a decentralized optimal control [27], a parallel distributed compensation for fuzzy system [28] and a hybrid system control [29]. Here the overlapping decomposition is applied to decompose the interconnected power systems by treating the tie-line as the overlapped variable.

Since the system (1) is a multi-input multi-output (MIMO) system, it is not easy to design frequency stabilizers directly from (1). To simplify the design process, the overlapping decomposition [18] is applied to extract the decoupled subsystem with single-input single-output (SISO) embedded with only the inter-area mode of interest. Accordingly, each frequency stabilizer can be individually designed in the decoupled subsystem.

First, decomposing the state variables into two groups, $z_1 = [x_1^t, x_2^t]^t$ and $z_2 = [x_2^t, x_3^t]^t$ with overlapping variable x_2, yields a new system with the vector $z = [z_1^t, z_2^t]^t$. The new

vector z is related to x by

$$z = Tx, \quad T = \begin{bmatrix} I_1 & 0 & 0 \\ 0 & I_2 & 0 \\ 0 & I_2 & 0 \\ 0 & 0 & I_3 \end{bmatrix}, \quad TT^I = I \tag{2}$$

where T is a nonsquare matrix of $(n_1 + 2n_2 + n_3) \times (n_1 + n_2 + n_3)$. I_1, I_2, I_3 are indentity matrices with dimensions corresponding to the components x_1, x_2, x_3 respectively. T^I is the generalized inverse of T. The linear transformation (2) defines the expansion system $\tilde{S}$ as

$$\tilde{S} : \overset{\bullet}{\tilde{z}} = \tilde{A}z + \quad \tilde{B}u \tag{3}$$

where $\tilde{A} = TAT^I + M$, $\tilde{B} = TB + N$, in which, matrices T^I , M and N are referred to

$$T^I = \begin{bmatrix} I_1 & 0 & 0 & 0 \\ 0 & 0.5I_2 & 0.5I_2 & 0 \\ 0 & 0 & 0 & I_3 \end{bmatrix}, \quad M = \begin{bmatrix} 0 & 0.5A_{12} & -0.5A_{12} & 0 \\ 0 & 0.5A_{12} & -0.5A_{22} & 0 \\ 0 & -0.5A_{22} & -0.5A_{22} & 0 \\ 0 & -0.5A_{32} & -0.5A_{32} & 0 \end{bmatrix}, \quad N = 0 \tag{4}$$

As a result, the expansion system $\tilde{S}$ can be described as

$$\tilde{S} : \begin{bmatrix} \dot{z}_1 \\ \dot{z}_2 \end{bmatrix} = \begin{bmatrix} A_{11} & A_{12} & 0 & A_{13} \\ A_{21} & A_{22} & 0 & A_{23} \\ A_{21} & 0 & A_{22} & A_{23} \\ A_{31} & 0 & A_{32} & A_{33} \end{bmatrix} \begin{bmatrix} z_1 \\ z_2 \end{bmatrix} + \begin{bmatrix} B_{11} & B_{12} \\ B_{21} & B_{22} \\ B_{21} & B_{22} \\ B_{31} & B_{32} \end{bmatrix} \begin{bmatrix} u_1 \\ u_2 \end{bmatrix} \tag{5}$$

Subsequently, the system $\tilde{S}$ can be decomposed into two interconnected overlapping subsystems, i.e.,

$$\tilde{S}_1 : \dot{z}_1 = \left(\begin{bmatrix} A_{11} & A_{12} \\ A_{21} & A_{22} \end{bmatrix} z_1 + \begin{bmatrix} B_{11} \\ B_{21} \end{bmatrix} u_1 \right) + \begin{bmatrix} 0 & A_{13} \\ 0 & A_{23} \end{bmatrix} z_2 + \begin{bmatrix} B_{12} \\ B_{22} \end{bmatrix} u_2 \tag{6}$$

and

$$\tilde{S}_2 : \dot{z}_2 = \left(\begin{bmatrix} A_{22} & A_{23} \\ A_{32} & A_{33} \end{bmatrix} z_2 + \begin{bmatrix} B_{21} \\ B_{31} \end{bmatrix} u_2 \right) + \begin{bmatrix} A_{21} & 0 \\ A_{31} & 0 \end{bmatrix} z_1 + \begin{bmatrix} B_{21} \\ B_{31} \end{bmatrix} u_1 \tag{7}$$

The state variable x_2 is repeatedly included in both subsystems, which implies "*Overlapping Decomposition*".

For system stabilization, the terms in the right hand sides of (6) and (7) can be separated into the decoupled subsystems (as indicated in the parenthesis in (6) and (7)) and the interconnected subsystems. As mentioned in [18], if each decoupled subsystem can be stabilized by its control input, the asymptotic stability of the original system S is also guaranteed. Consequently, the interactions between the decoupled subsystems and the interconnection subsystems in (6) and (7) are regarded as perturbations. They can be neglected in a design process. As a result, the decoupled subsystems can be expressed as

$$\tilde{S}_{D1} : \dot{z}_1 = \begin{bmatrix} A_{11} & A_{12} \\ A_{21} & A_{22} \end{bmatrix} z_1 + \begin{bmatrix} B_{11} \\ B_{21} \end{bmatrix} u_1 \tag{8}$$

$$\tilde{S}_{D2} : \dot{z}_2 = \begin{bmatrix} A_{22} & A_{23} \\ A_{32} & A_{33} \end{bmatrix} z_2 + \begin{bmatrix} B_{22} \\ B_{32} \end{bmatrix} u_2 \tag{9}$$

Each frequency stabilizer can be designed independently in (8) and (9). Here, the structure of frequency stabilizer is specified as the 2^{nd}-order lead/lag compensator as depicted in Figure 2. The controller parameters are tuned based on the proposed optimization in the next part.

3.2. **Formulation of optimization problem.** In deriving the optimization problem, not only the enhancement of system damping, but also the robust stability are taken into consideration. For the first purpose, the damping ratio (ζ) of the inter-area mode is used as a design specification. Assume that the eigenvalues corresponding to the oscillation mode are $-\sigma \pm j\omega_d$ and the damping ratio is given by

$$\zeta_{actual} = \frac{-\sigma}{\sqrt{\sigma^2 + \omega_d^2}} \tag{10}$$

The desired damping ratio is specified as $\zeta_{desired}$. Accordingly, the difference between the desired and the actual damping ratios can be defined as

$$\alpha = |\zeta_{desired} - \zeta_{actual}| \tag{11}$$

For robust stability, all possible uncertainties in power systems are represented by a multiplicative form [19], demonstrated in Figure 3. $\tilde{G}$ is a decoupled subsystem. $\tilde{K}$ is a frequency stabilizer. Δ_m is a stable multiplicative uncertainty.

To prove the robust stability condition for the system, first we need to find the transfer function seen by the uncertainty block. The input and output of this block are shown at the indicated points in Figure 4 (left) and its transfer function in Figure 4 (right) is

$$M(s) = \frac{\tilde{G}(s)\tilde{K}(s)}{1 + \tilde{G}(s)\tilde{K}(s)} \tag{12}$$

By the small-gain theorem [19], if the above transfer function and the uncertainty transfer function are stable, the system will be robustly stable if

$$|\Delta_m(s)M(s)| < 1 \tag{13}$$

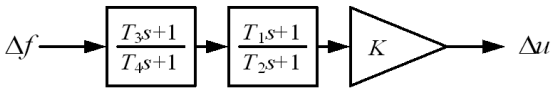

FIGURE 2. Structure of frequency stabilizer

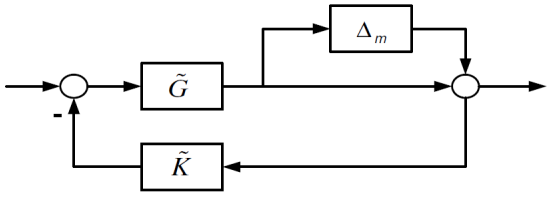

FIGURE 3. Feedback control system with multiplicative uncertainty

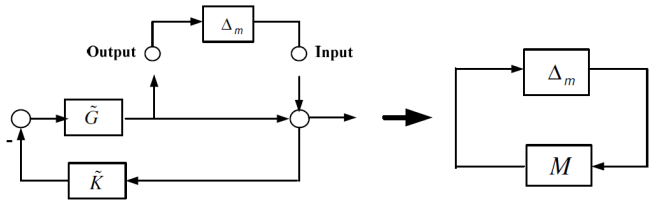

FIGURE 4. Obtaining the transfer function seen by the uncertainty (left) and the system as seen by the uncertainty (right)

Note that $|\bullet|$ is the magnitude of the transfer function "$\bullet$". Also, because of the following inequality

$$|\Delta_m M| \leq |\Delta_m|\,|M| \tag{14}$$

As a result, (14) becomes,

$$|\Delta_m|\,|M| \leq 1 \tag{15}$$

By substituting M, the closed-loop system will be robustly stable if

$$|\Delta_m| < \frac{1}{\left|\tilde{G}\tilde{K}\left(1+\tilde{G}\tilde{K}\right)^{-1}\right|} \tag{16}$$

where $\tilde{G}\tilde{K}(1+\tilde{G}\tilde{K})^{-1}$ is the complementary sensitivity function (T). As a result, the robust stability condition becomes

$$|\Delta_m| < \frac{1}{|T|} \tag{17}$$

In addition, the robust stability margin of the closed-loop system can be guaranteed in terms of multiplicative stability margin (MSM) as

$$\text{MSM} = 1/\left\|T\right\|_\infty \tag{18}$$

where $\left\|T\right\|_\infty$ is the ∞-norm of T. From (17) and (18), it is clear that by minimizing $\left\|T\right\|_\infty$, the MSM increases and the robust stability is ensured. Thus, the normalized robustness index of the objective function is defined as

$$\gamma = \left\|T\right\|_\infty \Big/ \left\|T\right\|_{\infty(initial)} \tag{19}$$

where $\left\|T\right\|_{\infty(initial)}$ is the ∞-norm of T at the initial of a search process. Combining (11) and (19), the control problem can be formulated as the following optimization problem

$$\begin{aligned} \text{Minimize} \quad & F(K,T_i) = c\cdot\alpha+\gamma \\ \text{Subject to} \quad & K_{\min} \leq K \leq K_{\max} \\ & T_{i,\min} \leq T_i \leq T_{i,\max}, \quad i=1,\ldots,4 \end{aligned} \tag{20}$$

where $F(K,T_i)$ is the objective function. The minimum and maximum values of the gain K are set to 0.1 and 5, respectively. The minimum and maximum values of the time constants T_i are set to 0.01 and 2, respectively. The constant coefficient c is used to weight α-term, so that $c\cdot\alpha$ dominates γ during the parameters optimization. Since γ is normalized to 1 at the initial solution, it is easy to find the value of c so that $c\cdot\alpha$ is greater than 1. Eventually, the search process minimizes both terms until $c\cdot\alpha$ meets the specification and γ decreases to the possible minimum value. All searched parameters are optimized by TS.

3.3. **Tabu search algorithm.** The TS which is proposed by Glover [28], is treated as the extremely promising heuristic algorithm for handling the combinatiorial optimization problems. It is an iterative procedure that begins from any initial solution and endeavors to find a better solution. Especially, the TS is characterized by its ability to avoid entrapment in a local optimal solution and prevent cycling by applying flexible memory of search history. In the past, the TS has been applied to solve electromagnetic optimization problem [29], a cluster building in wireless sensor networks [30] and a planning of secondary electric power distribution systems [31] etc. Here, the TS is applied to optimize the control parameters of frequency stabilizer. Hereafter, components of TS and the TS procedure are discussed.

3.3.1. *Encoding and decoding.* The concatenated encoding method is employed as shown in Figure 5. Each parameter is encoded in a binary string normalized over its range. This encoding method stacks each normalized string in series with each other to construct the string individual. The same number of nb bits is used to represent each parameter string.

On the other hand, a decoding scheme is carried out by converting encoded parameters to their actual values prior to the evaluation of objective function by

$$P_i = P_{i,\min} + \frac{B_i \times [P_{i,\max} - P_{i,\min}]}{2^{nb} - 1} \tag{21}$$

where P_i is the actual value of the i^{th} parameter, $P_{i,\max}$ and $P_{i,\min}$ are the maximum and minimum value of the i^{th} parameter. B_i is the decimal integer value of binary string of the i^{th} parameter. In this study, 16 bits are used to represent each parameter.

3.3.2. *Trial solution generation.* To generate a trial solution, one bit of a binary string of an initial solution is flipped at a time. Figure 6 conceptually illustrates the process. The maximum number of trial solutions in each iteration is referred to a neighborhood solution space (NS). In this paper, NS is set to 90 % of a total number of bits in a string individual ($\lfloor 0.9 \times nb \times NP \rfloor$) where NP is a number of searched parameters.

3.3.3. *Tabu list restriction.* Tabu List (TL) is utilized to keep attributes (bit positions) that created the best solution in the past iterations for iterations so that they cannot be used to create new solution candidates. Figure 7 shows the mechanism of TL. In this paper, the size of TL is determined by $\lfloor \sqrt{nb \times NP} \rfloor$.

3.3.4. *Aspiration level criterion.* The aspiration level (AL) criterion allows an attribute included in TL to override its tabu status if it leads to a more attractive solution. In particular, the AL is satisfied if the tabued attribute yields a solution that is better than the best solution reached at that iteration. After the AL is satisfied, updating TL is carried out by moving the tabued attribute back to the first position of the TL.

3.3.5. *Termination criteria.* The search process will terminate if the maximum allowable number of iterations is reached.

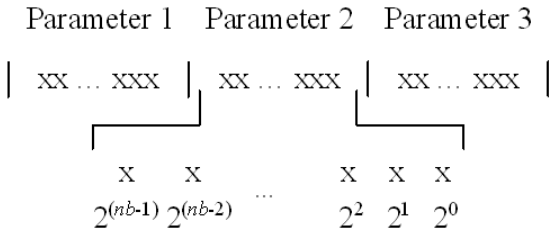

FIGURE 5. Example of concatenated encoding scheme

Initial solution :	1001011010	1100011010	1110010011
Trial solution 1:	0001011010	1100011010	1110010011
Trial solution 2:	1101011010	1100011010	1110010011
Trial solution 3:	1011011010	1100011010	1110010011

FIGURE 6. Concept of trial solution generation

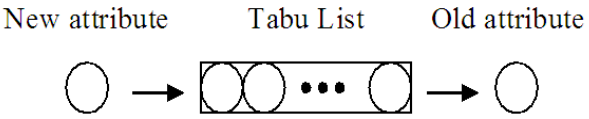

FIGURE 7. Mechanism of tabu list

3.3.6. *TS procedure.* Firstly, the initial feasible solution is generated arbitrarily. A trial solution is searched if either it is not tabued or, in case of being tabued it passes the AL test. The best solution is always updated during the search process until the termination criterion is satisfied. The following notations are used for the TS procedure.

$F(X)$: the objective function of solution X,
X_o^k: the initial feasible solution at iteration k,
X_m^k: a trial solution m at iteration k,
X_{cb}^k: the current best trial solution at iteration k,
X_b^k: the best solution reached at iteration k,
$k_{\max}$: the maximum allowable number of iterations.
The TS procedure can be described as follows.

1. Read constraints, the initial feasible solution X_o^k , and the design specification.
2. Specify the size of TL, $k_{\max}$, and size of NS.
3. Initialize iteration counter k and termination criteria tc to zero, and empty TL.
4. Initialized AL by setting $X_b^k = X_o^k$.
5. Execute TS procedure:
   5.1 Initialize the trial counter m to zero.
   5.2 Generate a trial solution X_m^k from X_o^k.
   5.3 If X_m^k is not feasible, go to 5.9.
   5.4 If X_m^k is the first feasible solution, set $X_{cb}^k = X_m^k$.
   5.5 Perform Tabu test. If X_m^k is tabued, then go to 5.8.
   5.6 If $F(X_m^k) < F(X_{cb}^k)$, set $X_{cb}^k = X_m^k$. Otherwise, go to 5.9.
   5.7 If $F(X_m^k) < F(X_b^k)$, then update AL by setting $X_b^k = X_m^k$. Go to 5.9.
   5.8 Perform AL test. If $F(X_m^k) < F(X_b^k)$, set $X_{cb}^k = X_m^k$, and update AL by setting $X_b^k = X_m^k$.
   5.9 If m is less than NS, $m = m + 1$ and go to 5.2.
   5.10 If there is no feasible solution, set $X_o^{k+1} = X_b^k$. Otherwise, set $X_o^{k+1} = X_{cb}^k$, and update TL.
6. If $k = 0$, go to 9.
7. Perform the convergence checking. If $X_b^k = X_b^{k-1}$, $tc = tc + 1$. Otherwise, $tc = 0$.
8. If $tc =$ size of TL, set $tc = 0$ and go to 10.
9. If $k < k_{\max}$, then $k = k + 1$, and go to 5.
10. TS is terminated and X_b^k is the best solution found.

The significance of the paper relative to previous works can be explained as follows.

1) The proposed optimization based on an enhancement of performance and robustness can be applied to tune frequency stabilizer of any power flow control devices. It not only improves the robust performance, but also guarantees the robust stability of the controller. This confirms the significance of this work in comparison with previous works [32,33] which did not take both objectives into account in the control design process.

2) The proposed optimization for any power flow devices can be applied to solve other frequency fluctuation problems in an interconnected power system with wind farm [34] and a microgrid with a hybrid wind/diesel generations [35], etc.

3) Not only the frequency stabilization problem, the proposed optimization can be applied to design power flow controllers for solving other power system problems such as an alleviation of power fluctuation in power systems due to wind power fluctuation [36] and a voltage control in microgrid [37].

4) The proposed robust controller is very practical for real power system since it is based on the 2^{nd}-order lead/lag compensator with single feedback. This simple and practical structure is very easy to implement in comparison with other complicated power controllers such as fuzzy control [38], neural network [39] and sliding model control [40] etc.

5) The proposed controller optimization can be applied to design controller with any specified structure such as PI and PID for application in an ultrasonic motors [41], a network cascade control system [42], a multivariable process [43] and a PID optimization [44] etc.

6) The proposed controller optimization can solve the difficulty of weight selection and high order control of H_∞ control design in the previous works such as a robust filter design [45], a tracking control [46], an uncertain nonlinear singular system [47] and a logic-based H_2/H_∞ control [48] etc.

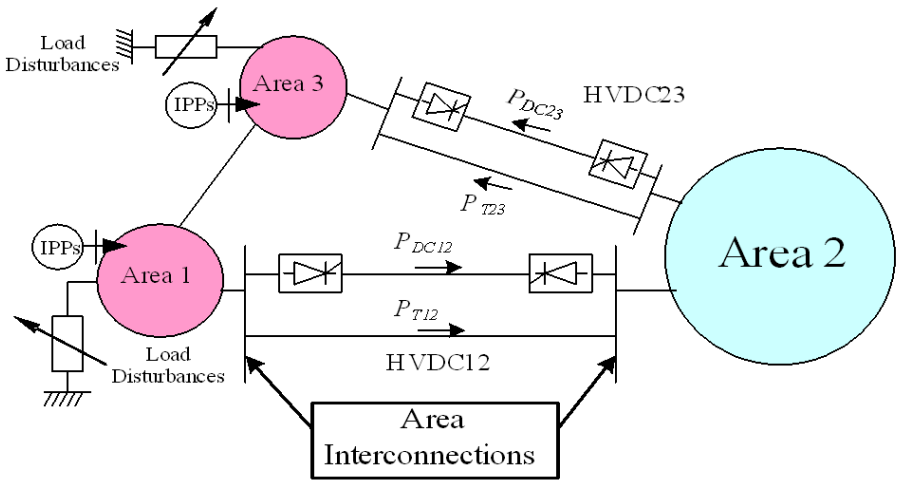

FIGURE 8. A three-area loop interconnected power system with two parallel AC-DC links

4. **Application 1: Frequency Stabilization by HVDC System.** A three-area loop system with two parallel AC-DC links shown in Figure 8 is used to show the proposed control design. HVDC12 and HVDC23 are connected in parallel with tie-lines between Areas 1 and 2, and Areas 2 and 3, respectively. It is assumed that large loads with sudden change have been placed in Areas 1 and 3. This causes a serious problem of frequency oscillations in both areas. In addition, the abilities of governors in both areas to provide frequency controls are not adequate. On the other hand, an Area 2 has a control capability enough to spare for other areas. Therefore, HVDC links are operated to employ the control capability of Area 2 to compensate for load changes in Areas 1 and 3. Besides, by utilizing the area interconnections as the channels of dynamic power flow control by HVDC links (P_{DC12} and P_{DC23}), both frequency oscillations in Areas 1 and 3 and tie-line power oscillations (P_{T12} and P_{T23}) due to inter-area modes can be effectively stabilized.

Since the response of HVDC link is extremely rapid when compared to a governor. For the sake of simplicity, a governor can be neglected in the design of frequency stabilizer. The linearized model of interconnected power system without governor can be shown in Figure 9. The HVDC link is represented by the first-order transfer function with time constant $T_{DC} = 0.05$s. The frequency stabilizers of HVDC12 and HVDC23 are expressed by $K_{12}(s)$ and $K_{23}(s)$, respectively. The configuration of each frequency stabilizer is based on a second-order lead/lag compensator depicted in Figure 2. The injected power deviation of each HVDC link (ΔP_{DC12} and ΔP_{DC23}) acting positively on an area reacts negatively on another area. Thus, each injected power simultaneously flows into interconnected areas with different signs $(+, -)$.

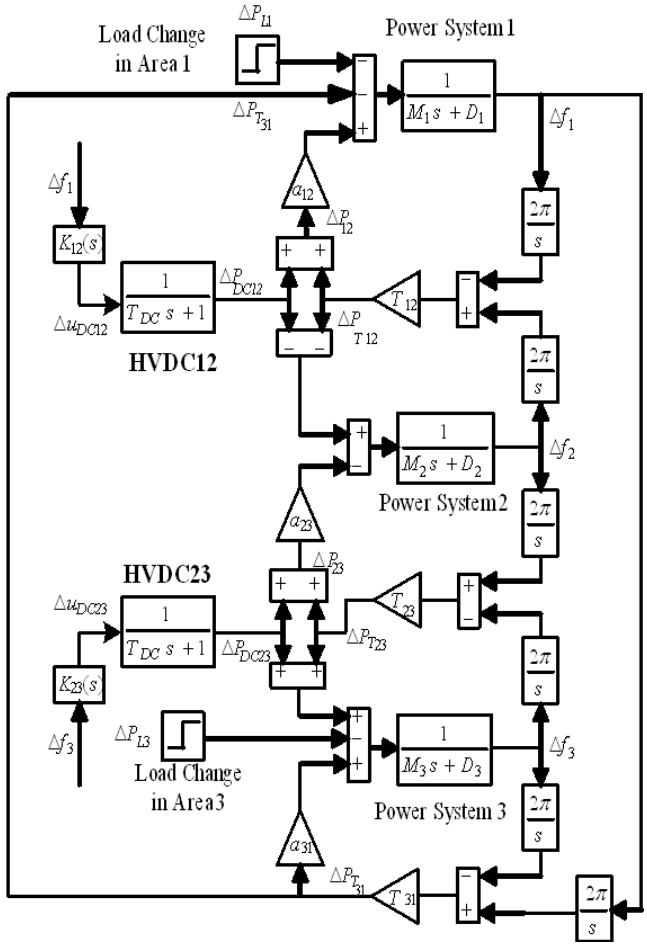

FIGURE 9. Linearized system without governors

By neglecting T_{DC}, the linearized state equation of system in Figure 8 is provided by

$$\Delta \dot{x} = A\Delta x + B\Delta u \tag{22}$$

where $\Delta x = \left[\begin{array}{ccccc} \Delta f_1 & \Delta P_{T12} & \Delta f_2 & \Delta P_{T23} & \Delta f_3 \end{array} \right]^T$, $\Delta u = \left[\begin{array}{cc} \Delta P_{DC12} & \Delta P_{DC23} \end{array} \right]^T$,

$$A = \left[\begin{array}{ccccc} -D_1/M_1 & a_{S12} & 0 & a_{S14} & 0 \\ -2\pi T_{12} & 0 & 2\pi T_{12} & 0 & 0 \\ 0 & -1/M_2 & -D_2/M_2 & -a_{23}/M_2 & 0 \\ 0 & 0 & 2\pi T_{23} & 0 & -2\pi T_{23} \\ 0 & a_{S52} & 0 & a_{S54} & -D_3/M_3 \end{array} \right]$$

$$B = \begin{bmatrix} a_{12}/M_1 & 0 \\ 0 & 0 \\ -1/M_2 & -a_{23}/M_2 \\ 0 & 1/M_3 \\ 0 & 0 \end{bmatrix}$$

where Δf_i is the frequency deviation of area i, ΔP_{Tij} is the AC tie-line power deviation between areas i and j, ΔP_{DCij} is an injected power of HVDC link between areas i and j. ΔP_{ij} is a total tie-line power deviations ($\Delta P_{Tij} + \Delta P_{DCij}$), M_i is the inertia constant of area i, D_i is the damping coefficient of area i, a_{ij} is the area capacity ratio between areas i and j, T_{ij} is the synchronizing power coefficient between areas i and j, where $i, j = 1, \ldots, 3$. Here $a_{S12} = (a_{12} + T_{31}/T_{12})/M_1$, $a_{S14} = -T_{31}/(M_1 T_{23})$, $a_{S52} = -a_{31}T_{31}/(M_3 T_{12}), a_{S54} = (1 + a_{31}T_{31}/T_{23})/M_3$.

This system has two conjugate pairs of complex eigenvalues and a negative real eigenvalue. The former corresponds to two inter-area oscillation modes, and the latter the inertia center mode. Based on the mode controllability matrix [1], it can be verified that the inter-area modes between Areas 1 and 2, and Areas 2 and 3 are controllable for the control inputs Δu_{DC12} and Δu_{DC23}, respectively. Accordingly, the purpose of each frequency stabilizer is to improve the damping of the target inter-area mode. By regarding the tie-line power deviation between Areas 1 and 2 (ΔP_{T12}) as the overlapped variable for design of frequency stabilizer of HVDC12, the subsystem embedded with the inter-area mode between Areas 1 and 2 can be shown as

$$\tilde{G}_{S1} : \begin{bmatrix} \Delta \dot{f}_1 \\ \Delta \dot{P}_{T12} \end{bmatrix} = \begin{bmatrix} -D_1/M_1 & a_{S12} \\ -2\pi T_{12} & 0 \end{bmatrix} \begin{bmatrix} \Delta f_1 \\ \Delta P_{T12} \end{bmatrix} + \begin{bmatrix} a_{12}/M_1 \\ 0 \end{bmatrix} \Delta P_{DC12} \tag{23}$$

Next, by considering the tie-line power deviation between Areas 2 and 3 (ΔP_{T23}) as the overlapped variable for design of frequency stabilizer of HVDC23, the subsystem included with the inter-area mode between Areas 2 and 3 can be expressed as

$$\tilde{G}_{S2} : \begin{bmatrix} \Delta \dot{P}_{T23} \\ \Delta \dot{f}_3 \end{bmatrix} = \begin{bmatrix} 0 & -2\pi T_{23} \\ a_{S54} & -D_3/M_3 \end{bmatrix} \begin{bmatrix} \Delta P_{T23} \\ \Delta f_3 \end{bmatrix} + \begin{bmatrix} 0 \\ 1/M_3 \end{bmatrix} \Delta P_{DC23} \tag{24}$$

By incorporating the time constant of the HVDC link, (22) and (23) become

$$G_{S1} : \begin{bmatrix} \Delta \dot{f}_1 \\ \Delta \dot{P}_{T12} \\ \Delta \dot{P}_{DC12} \end{bmatrix} = \begin{bmatrix} -D_1/M_1 & a_{S12} & a_{12}/M_1 \\ -2\pi T_{12} & 0 & 0 \\ 0 & 0 & -1/T_{DC12} \end{bmatrix} \begin{bmatrix} \Delta f_1 \\ \Delta P_{T12} \\ \Delta P_{DC12} \end{bmatrix} + \begin{bmatrix} 0 \\ 0 \\ 1/T_{DC12} \end{bmatrix} \Delta u_{DC12} \tag{25}$$

$$G_{S2} : \begin{bmatrix} \Delta \dot{P}_{T23} \\ \Delta \dot{f}_3 \\ \Delta \dot{P}_{DC23} \end{bmatrix} = \begin{bmatrix} 0 & -2\pi T_{23} & 0 \\ a_{S54} & -D_3/M_3 & 1/M_3 \\ 0 & 0 & -1/T_{DC23} \end{bmatrix} \begin{bmatrix} \Delta P_{T23} \\ \Delta f_3 \\ \Delta P_{DC23} \end{bmatrix} + \begin{bmatrix} 0 \\ 0 \\ 1/T_{DC23} \end{bmatrix} \Delta u_{DC23} \tag{26}$$

where Δu_{DC12} and Δu_{DC23} are output signals of frequency stabilizers for HVDC12 and HVDC23, respectively. Equations (25) and (26) are used to design frequency stabilizers of HVDC12 and HVDC23, respectively. The frequency deviation of the target area ($\Delta f_i, i =$ 1 and 3) which provides information of each inter-area oscillation mode, is used as the

input signal for each frequency stabilizer. The control parameters in Figure 2 which consist of a stabilization gain K, time constants T_1, T_2, T_3 and T_4 are optimized via the objective function (20).

In this study, the desired damping ratio ($\zeta_{desired}$) is set to 0.25. Also, the coefficient c is appropriately set to 5. For TS, the size of TL is set to 8. The tuned parameters of each stabilizer are obtained in Table 1. The resulted frequency stabilizer is referred to as "Robust frequency stabilizer". For comparison purpose, each frequency stabilizer is optimized by ignoring γ-term and setting $c = 1$ in (20). With the same $\zeta_{desired}$, the resulted frequency stabilizer is referred to as "Non-robust frequency stabilizer". Control parameters of Non-robust frequency stabilizers are also given in Table 1.

Table 2 shows eigenvalues corresponding to the inter-area modes of subsystems (25) and (26). The analysis results describe that the damping ratios of the inter-area modes in cases of Robust and Non-robust frequency stabilizers are improved to 0.25 as design specification.

Next, the MSM is used to evaluate the robust stability margins of (25) and (26) installed with designed frequency stabilizer. As shown in Table 3, the values of MSM in case of robust frequency stabilizers are greater than those in case of non-robust stabilizers.

The performance and robustness of frequency stabilizers are evaluated in a linearized three-area interconnected system. The dynamic of governor [1] as illustrated in Figure 10 is also incorporated in each area. In the simulation study, load disturbances which are simultaneously applied to Areas 1 and 3, are composed of three different components of oscillating frequency as

$$\text{Area } 1 : \Delta P_{L1} = 0.003 \sin(4.36t) + 0.005 \sin(5.3t) - 0.007 \sin(6t) \tag{27}$$

$$\text{Area } 3 : \Delta P_{L3} = 0.003 \sin(3.29t) + 0.007 \sin(4t) - 0.005 \sin(4.5t) \tag{28}$$

As demonstrated in Figures 11 and 12, both load disturbances cause severe frequency oscillations in case of HVDCs with no frequency stabilizers. On the other hand, frequency oscillations are significantly damped in case of HVDCs with either robust or non-robust frequency stabilizers.

TABLE 1. Control parameters of robust and non-robust frequency stabilizers

Robust Frequency Stabilizers	K	T_1	T_2	T_3	T_4
HVDC12	0.2188	0.2587	0.0158	0.0575	0.2316
HVDC23	0.2378	1.5025	0.5386	1.6268	0.5075
Non-robust Frequency Stabilizers	K	T_1	T_2	T_3	T_4
HVDC12	4.2863	0.1344	1.0011	1.0978	1.3807
HVDC23	4.3683	0.1344	0.9933	1.3467	1.3802

TABLE 2. Comparison of eigenvalues of subsystems

Subsystem (equation)	HVDCs without Frequency Stabilizers	HVDCs with Non-Frequency Robust Stabilizers	HVDCs with Robust Frequency Stabilizers
(25)	$-0.015 \pm j3.53$, $\zeta = 0.004$	$-1.84 \pm j7.11$, $\zeta = 0.25$	$-0.61 \pm j2.36$, $\zeta = 0.25$
(26)	$-0.016 \pm j3.31$, $\zeta = 0.005$	$-1.67 \pm j6.46$, $\zeta = 0.25$	$-0.35 \pm j1.36$, $\zeta = 0.25$

TABLE 3. Comparison of MSM

Subsystem (equation)	HVDCs with Non-Robust Frequency Stabilizers	HVDCs with Robust Frequency Stabilizers
(25)	0.5151	0.9143
(26)	0.5332	0.9024

Here, it is assumed that both systems are unstable so that D_1 and D_3 are set -0.45 pu.MW/Hz. Frequency oscillations in case of HVDCs with non-robust frequency stabilizers severely fluctuate and finally diverge as depicted in Figures 13 and 14. On the contrary, frequency oscillations are considerably damped by HVDCs with robust frequency stabilizers. Simulation results confirm the high robustness of the robust frequency stabilizers.

5. **Application 2: Frequency Stabilization by SMES.** A typical two-area interconnected power system shown in Figure 15 is used for frequency stabilization studies.

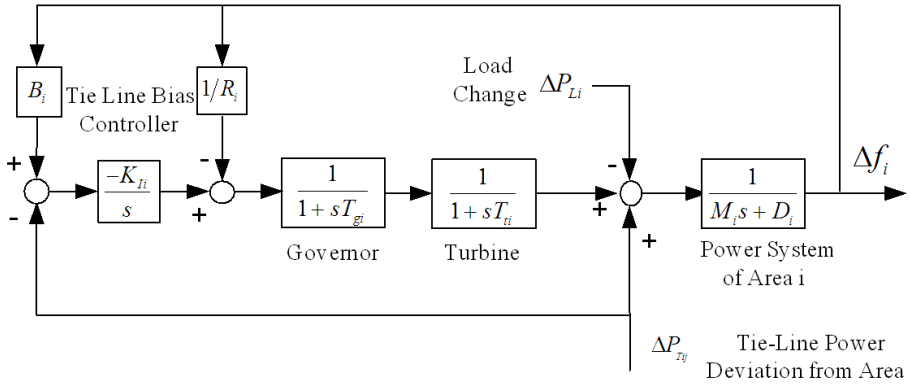

FIGURE 10. Linearized system of area i including governor

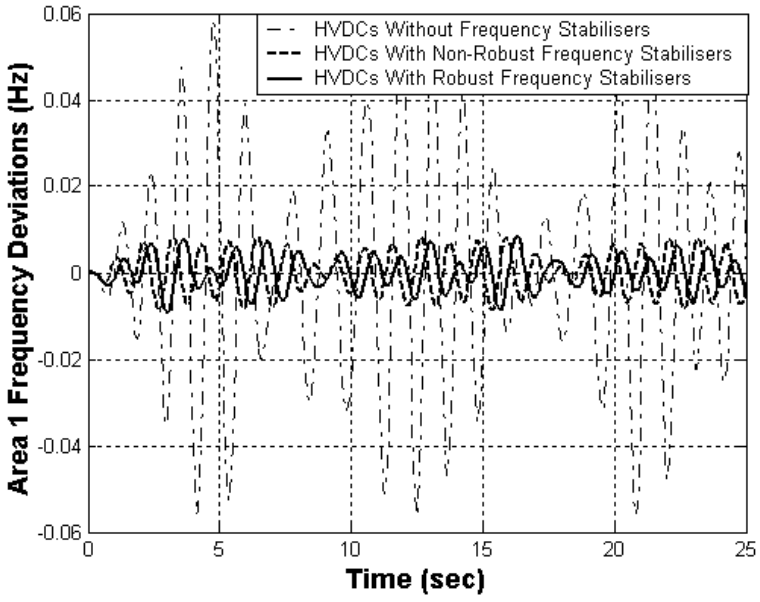

FIGURE 11. Frequency oscillations of Area 1

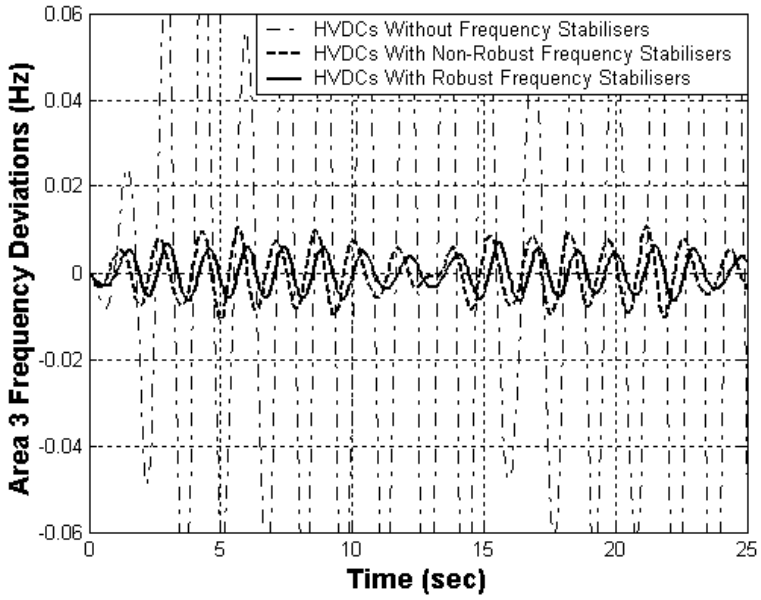

FIGURE 12. Frequency oscillations of Area 3

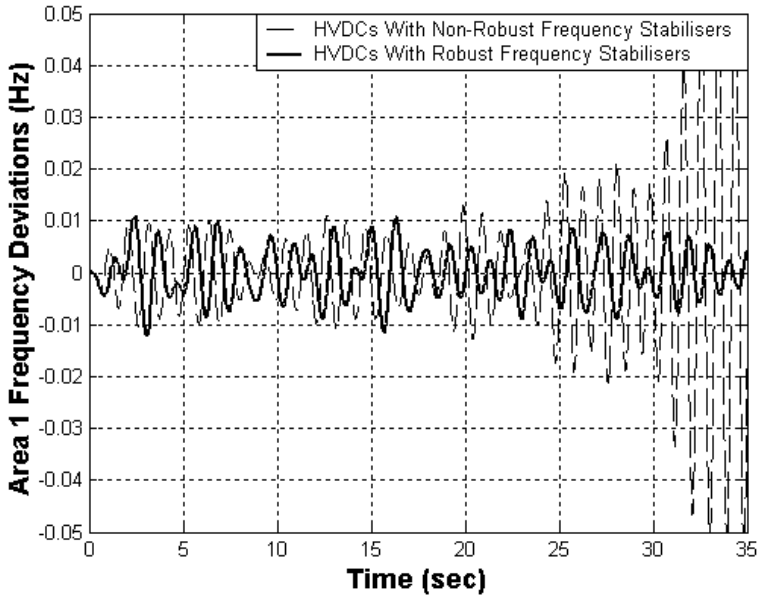

FIGURE 13. Frequency oscillations of Area 1

SMES1 and SMES2 are installed at the terminal buses of Areas 1 and 2, respectively. The linearized model [49] including the reheat steam turbine, boiler and deadband is depicted in Figure 16. In the design specification, the desired damping ratio ($\zeta_{desired}$) is set to 0.25. The coefficient c in (20) is appropriately set to 5.

Based on the design procedure, control parameters of robust and non-robust frequency stabilizers are provided in Table 4. Note that, since both areas are identical, control parameters of frequency stabilizers of SMES1 are the same as those of SMES2.

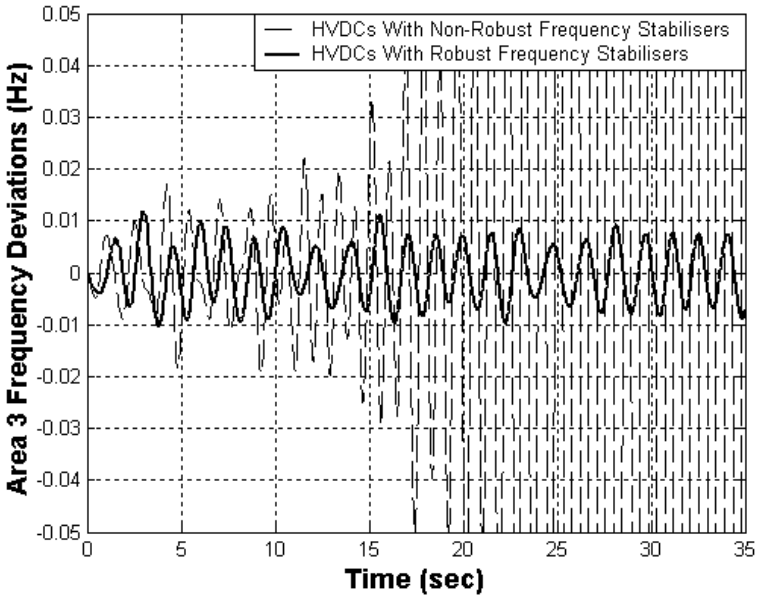

FIGURE 14. Frequency oscillations of Area 3

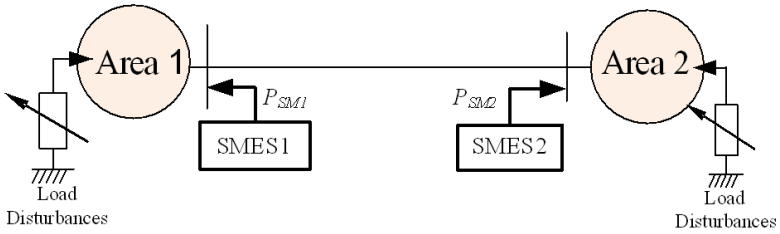

FIGURE 15. A two-area interconnected power system with two units of SMES

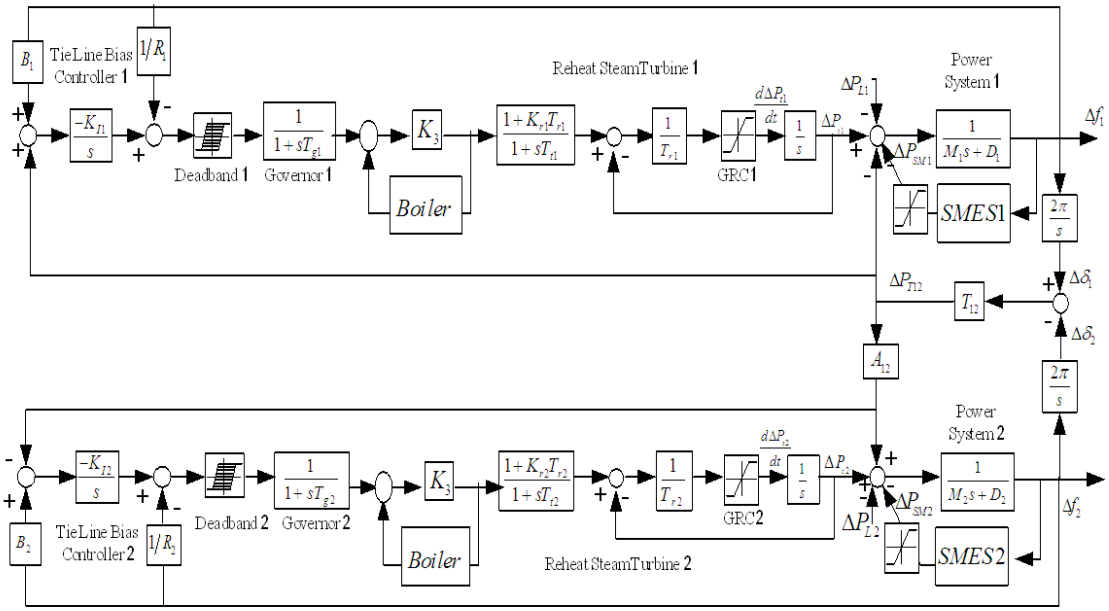

FIGURE 16. A two-area interconnected power system with two units of SMES

TABLE 4. Control parameters of robust/non-robust frequency stabilizers

Control Parameters of SMES1 and SMES2	K	T_1	T_2	T_3	T_4
Robust Frequency Stabilizers	2.6167	0.1987	1.5023	1.0203	1.4742
Non-robust Frequency Stabilizers	2.7872	0.1364	1.5024	1.0979	1.4120

TABLE 5. Comparison of eigenvalues

Without SMESs	SMESs With Non-Robust Frequency Stabilizers	SMESs With Robust Frequency Stabilizers
$-0.025 \pm j1.63$ $\zeta = 0.0153$	$-0.86 \pm j3.33$ $\zeta = 0.25$	$-0.8 \pm j3.1$ $\zeta = 0.25$

Eigenvalue anlaysis results are declared in Table 5. The damping ratio of inter-area mode is enhanced to 0.25 as design specification in either case of robust or non-robust frequency stabilizers.

In a simulation study, load disturbances with changing frequency of inter-area mode are applied as

$$\text{Area } 1 : \Delta P_{L1} = 0.007 \sin(1.63t) \tag{29}$$

$$\text{Area } 2 : \Delta P_{L2} = -0.008 \sin(1.63t) \tag{30}$$

The effects of frequency stabilization of SMES1 and SMES2 on Areas 1 and 2 are shown in Figures 17 and 18, respectively. Both robust and non-robust frequency stabilizers are able to damp frequency oscillations. Note that frequency oscillations by both types of frequency stabilizer are almost the same.

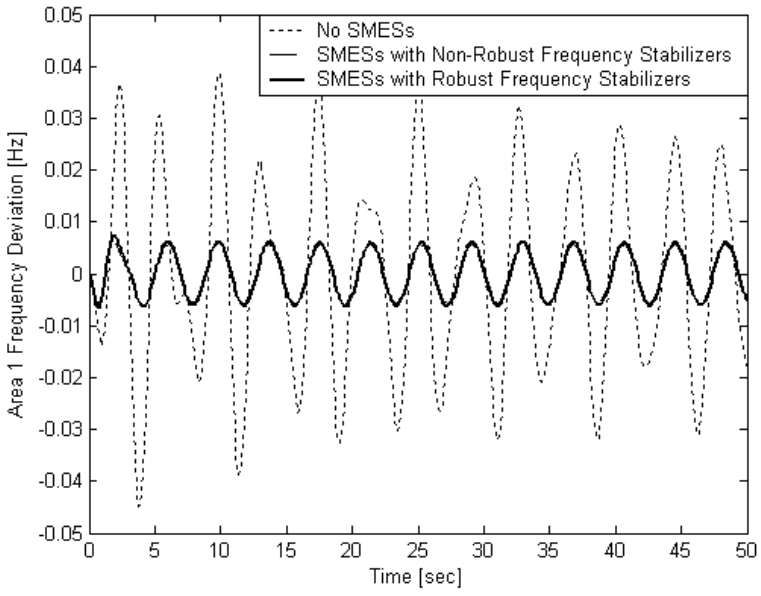

FIGURE 17. Frequency oscillations of Area 1

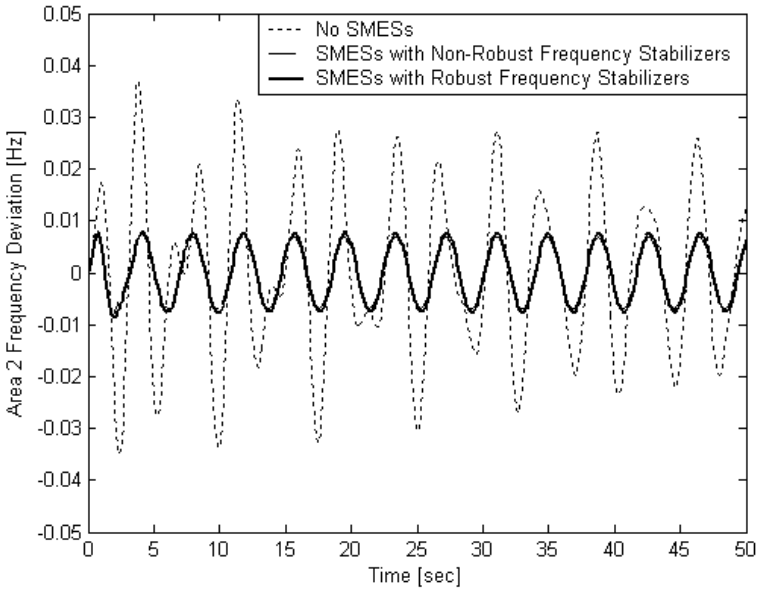

FIGURE 18. Frequency oscillations of Area 2

To evaluate the robustness of frequency stabilizers, load disturbances (29) and (30) are applied to Areas 1 and 2, respectively, while the damping coefficients of both areas are changed to -0.2 [puMW/Hz]. As depicted in Figures 19 and 20, frequency oscillations of both areas, severely oscillate and diverge in case of SMESs with non-robust frequency stabilizers. On the other hand, frequency oscillations are significantly damped by SMESs with robust frequency stabilizers.

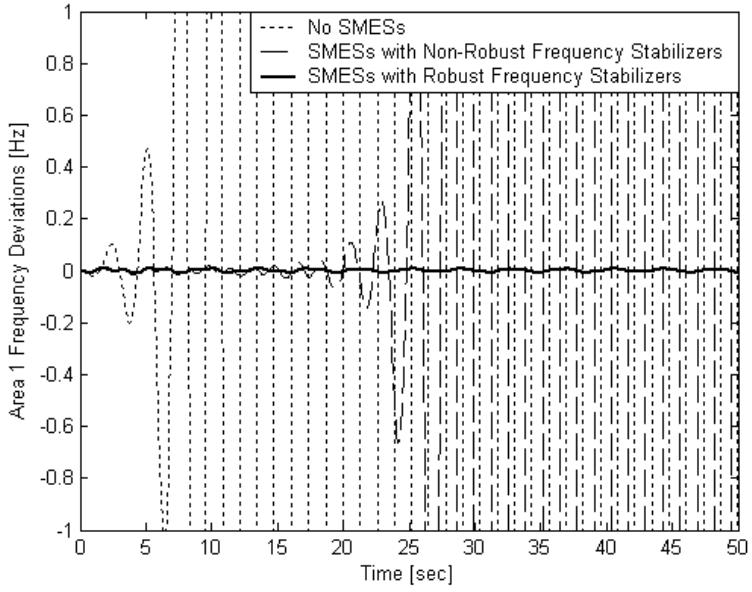

FIGURE 19. Frequency oscillations of Area 1

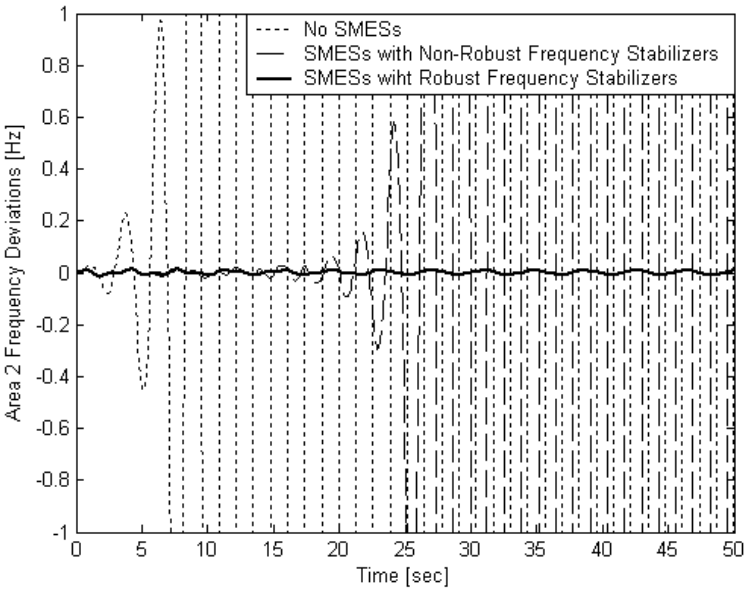

FIGURE 20. Frequency oscillations of Area 2

To present a truly significant and novel contribution, the advantages of the current work compared with existing results in literatures are provided as follows.

1) The proposed method applies the overlapping decompositions to decompose the original system with overlapping structure. As a result, the controller optimization can be carried out independently in each subsystem. The overlapping decompositions not only simplify the optimization but also assure the system stability. In terms of the simple control design, the cost of realization and reliability, the proposed technique is much superior to previous works which present frequency control designs of SMES [50,51] and HVDC [52] by the original system with high order.

2) Based on the enhancement of robust stability margin of multiplicative uncertainty model, the proposed controller is very robust against system uncertainties such as random load changes, system parameters variation and system nonlinearities etc. The high robustness of the proposed controller has never considered in the previous design of SMES [53] and HVDC [54]. As a result, the controllers in [53,54] may fail to stabilize frequency oscillation when the system uncertainties are high.

3) The structure of the controller is a practical 2^{nd}-order lead-lag compensator in comparison with the complicated structure of the state feedback based HVDC [52], a sliding mode control-based HVDC [55], a fuzzy control-based SMES [56] and an H_∞ control-based SMES [57], etc. Accordingly, the proposed controller is easy to realize in practical power systems.

4) The tabu search optimization based on the concept of enhancement of robust stability margin against system uncertainty by multiplicative uncertainty model provides a new contribution in H_∞ control design. It can overcome the difficulty of weighting function tuning and a problem of controller with high order as such as an H_∞ control-based SMES [57] and a mixed H_2/H_∞ control-based SMES [58].

5) The proposed robust control design is carried out in the system model considering uncertainties due to system parameters variation. Without exact mathematic equations,

the multiplicative perturbation can be applied to represent all possible unstructured uncertainties in the proposed model. This developed model not only simplifies the representation of system uncertainties, but also makes the control design practically and conveniently. This merit of the proposed design overcomes the difficulty of uncertainty modeling in [59,60].

6. **Conclusion.** A new robust decentralized fixed structure H_∞ frequency stabilizer design based on overlapping decomposition for frequency stabilization in interconnected power systems has been presented. The overlapping decomposition is applied to extract the designed subsystem embedded with the target inter-area mode from the original system. By including the multiplicative uncertainty in the designed subsystem, the optimization problem which considers both damping effects and robust stability, can be formulated. To achieve both performance and robustness, the control parameters of frequency stabilizer are optimized by a tabu search. Two examples of frequency stabilization by HVDC and SMES are used to demonstrate the effect of the proposed control design. Simulation studies have confirmed the high robustness of frequency stabilizers of HVDC and SMES against load disturbances, system parameter variations and negative damping.

Acknowledgement. This work was supported by the King Mongkut's Institute of Technology Ladkrabang Research Fund.

REFERENCES

[1] P. Kundur, *Power System Stability and Control*, McGraw Hill, 1994.
[2] G. Rogers, *Power System Oscillations*, Kluwer Acaemic, 2000.
[3] N. Jaleeli, L. S. VanSlyck, D. N. Ewart, L. H. Fink and A. G. Hoffmann, Understanding automatic generation control, *IEEE Transactions on Power Systems*, vol.7, no.3, pp.1106-1122, 1999.
[4] J. Pahasa and I. Ngamroo, Least square support vector machine for power system stabilizer design using wide area phasor measurements, *International Journal of Innovative Computing, Information and Control*, vol.7, no.7(B), pp.4487-4501, 2011.
[5] M. M. Al-Harthi, Robust AVR design based on mixed H_2/H_∞ pole placement using linear matrix inequality (LMI), *ICIC Express Letters*, vol.4, no.3(B), pp.963-971, 2010.
[6] H. F. Wang, F. J. Swift and M. Li, Comparison of modal controllability between FACTS-based stabilizers and PSS in increasing the oscillation stability of multimachine power systems, *IEE Proceedings Generation, Transmission and Distribution*, vol.143, no.6, pp.1350-1360, 1996.
[7] M. A. Abido, Simulated annealing based approach to PSS and FACTS based stabilizer tuning, *International Journal of Electrical Power & Energy Systems*, vol.22, no.4, pp.247-258, 2000.
[8] L. Y. Sun, J. Zhao and G. M. Dimirovski, Nonlinear robust controller design for thyristor controlled series compensation, *International Journal of Innovative Computing, Information and Control*, vol.5, no.4, pp.981-989, 2009.
[9] C.-K. Kim, V. K. Sood, G.-S. Jang, S.-J. Lim and S.-J. Lee, *HVDC Transmission: Power Conversion Applications in Power Systems*, Wiley-IEEE Press, 2009.
[10] M. Sanpei, A. Kakehi and H. Takeda, Application of multi-variable control for automatic frequency controller of HVDC transmission system, *IEEE Transactions on Power Delivery*, vol.9, no.2, pp.1063-1068, 1994.
[11] T. S. Chung and F. D. Zhong, Fuzzy logic controller for enhancing oscillatory stability of AC-DC interconnected power system, *Electric Power System Research*, vol.61, no.3, pp.221-226, 2002.
[12] T. Chaiyatham and I. Ngamroo, Optimal fuzzy gain scheduling of PID controller of superconducting magnetic energy storage for power system stabilization, *International Journal of Innovative Computing, Information and Control*, (in press).
[13] S. C. Tripathy, R. Balasubramanian and P. S. C. Nair, Adaptive automatic generation control with superconducting magnetic energy storage in power systems, *IEEE Transactions Energy Conversions*, vol.7, no.3, pp.434-441, 1992.
[14] A. Demiroren, H. L. Zeynelgil and N. S. Sengor, Automatic generation control for power system with SMES by using neural network controller, *Electric Power Components and Systems*, vol.31, no.1, pp.1-25, 2003.

[15] A. Demiroren and E. Yesil, Automatic generation control with fuzzy logic controllers in the power system including SMES units, *International Journal of Electrical Power and Energy Systems*, vol.26, no.4, pp.291-305, 2004.
[16] C. Y. Chen and G. T. C. Chiu, H_∞ robust controller design of media advance systems with time domain specifications, *International Journal of Innovative Computing, Information and Control*, vol.4, no.4, pp.813-828, 2008.
[17] S. Kaitwanidvilai, P. Olarnthichachart and I. Ngamroo, PSO based automatic weight selection and fixed structure robust loop shaping control for power system control applications, *International Journal of Innovative Computing, Information and Control*, vol.7, no.4, pp.1549-1563, 2011.
[18] M. Ikeda, D. D. Siljak and D. E. White, Decentralized control with overlapping information sets, *Journal of Optimization Theory and Applications*, vol.34, no.2, pp.279-310, 1981.
[19] S. Skogestad and I. Postlethwaite, *Multivariable Feedback Control: Analysis and Design*, John Wiley and Sons Ltd., 2005.
[20] F. Glover and M. Laguna, *Tabu Search*, Kluwer Academic Publishers, 2000.
[21] W. S. Levine and M. Athans, On the optimal error regulation of a string of moving vehicles, *IEEE Transactions on Automatic Control*, vol.11, pp.255-361, 1966.
[22] M. Aoki, On decentralized stabilization and dynamic assignment problems, *Journal International Economics*, vol.6, pp.143-174, 1976.
[23] M. S. Calovic, Automatic generation control: decentralized area-wise optimal solution, *Electric Power Systems Research*, vol.7, pp.115-139, 1984.
[24] D. D. Siljak, *Large-Scale Dynamic Systems: Stability and Structure*, North-Holland, 1978.
[25] M. Ikeda and D. D. Siljak, Overlapping decompositions, expansions and contractions of dynamic systems, *Large Scale Systems*, vol.1, pp.29-38, 1980.
[26] M. Akar and U. Ozgner, Decentralized techniques for the analysis and control of Takagi-Sugeno fuzzy systems, *IEEE Transactions on Fuzzy Systems*, vol.8, pp.691-704, 2000.
[27] A. Iftar and U. Ozgner, Overlapping decompositions, expansions, contractions and stability of hybrid systems, *IEEE Transactions on Automatic Control*, vol.43, pp.1040-1055, 1998.
[28] F. Glover, A user's guide to tabu search, *Annual Operation Research*, vol.41, pp.3-28, 1993.
[29] S. Carcangiu, A. Fanni, A. Mereu and A. Montisci, Grid-enabled tabu search for electromagnetic optimization problems, *IEEE Transactions on Magnetics*, vol.46, no.8, pp.3265-3268, 2010.
[30] A. Elrhazi and S. Pierre, A tabu search algorithm for cluster building in wireless sensor networks, *IEEE Transactions on Mobile Computing*, vol.8, no.4, pp.433-444, 2009.
[31] A. M. Cossi, R. Rornero and J. R. S. Mantovani, Planning and projects of secondary electric power distribution systms, *IEEE Transactions on Power Systems*, vol.24, no.3, pp.1599-1608, 2009.
[32] P. Bhatt, R. Roy and S. P. Ghoshal, Comparative performance evaluation of SMES-SMES, TCPS-SMES and SSSC-SMES controllers in automatic generation control for a two-area hydro-hydro system, *International Journal of Electrical Power & Energy Systems*, vol.33, no.10, pp.1585-1597, 2011.
[33] P. Bhatt, R. Roy and S. P. Ghoshal, Load frequency stabilization by coordinated control of thyristor controlled phase shifters and superconducting magnetic energy storage for three types of interconnected two-area power systems, *International Journal of Electrical Power & Energy Systems*, vol.32, no.10, pp.1111-1124, 2010.
[34] P. Bhatt, S. P. Ghoshal and R. Roy, Coordinated control of TCPS and SMES for frequency regulation of interconnected restructured power systems with dynamic participation from DFIG based wind farm, *Renewable Energy*, vol.40, no.1, pp.40-50, 2012.
[35] M. Md. T. Ansari and S. Velusami, Dual mode linguistic hedge fuzzy logic controller for an isolated wind-diesel hybrid power system with superconducting magnetic energy storage unit, *Energy Conversion and Management*, vol.51, no.1, pp.169-181, 2010.
[36] I. Ngamroo, Robust SMES controller design based on inverse additive perturbation hybrid for stabilization of interconnected power systems with wind farms, *Energy Conversion and Management*, vol.51, no.3, pp.459-464, 2010.
[37] S. Vachirasricirikul, I. Ngamroo and S. Kaitwanidvilai, Coordinated SVC and AVR for robust voltage control in a hybrid wind-diesel system, *Energy Conversion and Management*, vol.51, no.12, pp.2383-2393, 2010.
[38] A. M. Hemeida, A fuzzy logic controlled superconducting magnetic energy storage, SMES frequency stabilizer, *Electric Power Systems Research*, vol.80, no.6, pp.651-656, 2010.
[39] A. Demiroren, H. L. Zeynelgil and N. S. Sengor, The application of NN technique to automatic generation control for the power system with three areas including SMES units, *European Transactions on Electrical Power*, vol.13, no.4, pp.227-238, 2003.

[40] D. Qian, J. Yi and X. Liu, Sliding mode technology for automatic generation control of single area power systems, *ICIC Express Letters*, vol.5, no.8(A), pp.2415-2421, 2011.
[41] Y. Wakasa, S. Kanagawa, K. Tanaka and Y. Nishimura, A controller parameter tuning method considering dead-zone and saturation and its application to ultrasonic motors, *ICIC Express Letters, Part B: Applications*, vol.3, no.2, pp.265-270, 2012.
[42] C. Huang and Y. Bai, Tuning of PID controllers for networked cascade control systems with universal configurations, *ICIC Express Letters*, vol.6, no.7, pp.1857-1864, 2012.
[43] R. C. Panda and M. O. Tade, A Smith predictor with PID structure for control of multivariable processes, *ICIC Express Letters, Part B: Applications*, vol.1, no.2, pp.99-105, 2010.
[44] T. Wang, J. Wang, H. Peng and M. Tu, Optimization of PID controller parameters based on PSOPS algorithm, *ICIC Express Letters*, vol.6, no.1, pp.273-280, 2012.
[45] J. Qiu, X. Zhu, L. Su and Y. Wang, Robust H-infinity guaranteed cost filter design for a class of uncertain nonlinear time-delay stochastic system, *ICIC Express Letters*, vol.5, no.4(B), pp.1227-1233, 2011.
[46] J. Kang, Networked H-infinity output tracking control based QoS, *ICIC Express Letters*, vol.5, no.4, pp.945-952, 2011.
[47] J. Qiu, Y. Wang, X. Du, Y. Zhao and Y. Guo, Robust H-infinity control for uncertain nonlinear singular systems with time-varying delay, *ICIC Express Letters*, vol.5, no.2, pp.299-304, 2011.
[48] F. Jamshidi, M. G. Moghadam and M. T. H. Beheshti, Synthesis of a logic-based switching H_2/H_∞ controller: An intelligent supervisor approach, *ICIC Express Letters*, vol.4, no.1, pp.7-12, 2010.
[49] S. C. Tripathy, R. Balasubramanian and P. S. C. Nair, Effect of superconducting magnetic energy storage on automatic generation control considering governor deadband and boiler dynamics, *IEEE Transactions on Power Systems*, vol.7, no.3, pp.1266-1273, 1992.
[50] S. C. Tripathy and K. P. Juengst, Sampled data automatic generation control with superconducting magnetic energy storage in power systems, *IEEE Transactions on Energy Conversion*, vol.12, no.2, pp.187-192, 1997.
[51] S. Banerjee, J. K. Chatterjee and S. C. Tripathy, Application of magnetic energy storage unit as load-frequency stabilizer, *IEEE Transactions on Energy Conversion*, vol.5, no.1, pp.46-51, 1990.
[52] I. Ngamroo, A stabilization of frequency oscillation in a parallel AC-DC interconnected power system via an HVDC link, *Science Asia*, vol.28, no.2, pp.173-180, 2002.
[53] I. Ngamroo, Y. Mitani and K. Tsuji, Application of SMES coordinated with solid-state phase shifter to LFC, *IEEE Transactions on Applied Superconductivity*, vol.9, no.2, pp.322-325, 1999.
[54] S. Ganapathy and S. Velusami, MOEA based design of decentralized controllers for LFC of interconnected power systems with nonlinearities, AC-DC parallel tie-lines and SMES units, *Energy Conversion and Management*, vol.51, no.5, pp.873-880, 2010.
[55] K. Y. Kim, Y. Wang and R. Zhou, Decentralised robust load-frequency control in coordination with frequency controllable HVDC, *International Journal of Electrical Power & Energy Systems*, vol.19, no.7, pp.423-431, 1997.
[56] S. Pothiya and I. Ngamroo, Optimal fuzzy logic-based PID controller for load-frequency control including superconducting magnetic energy storage units, *Energy Conversion and Management*, vol.49, no.10, pp.2833-2838, 2008.
[57] I. Ngamroo, C. Taeratanachai, S. Dechanupaprittha and Y. Mitani, Enhancement of load frequency stabilization effect of superconducting magnetic energy storage by static synchronous series compensator based on H_∞ control, *Energy Conversion and Management*, vol.48, no.4, pp.1302-1312, 2007.
[58] H. Shayeghi, A. Jalili and H. A. Shayanfar, A robust mixed H_2/H_∞ based LFC of a deregulated power system including SMES, *Energy Conversion and Management*, vol.49, no.10, pp.2656-2668, 2008.
[59] H. Bevrani, Y. Mitani and K. Tsuji, Robust decentralized AGC in a restructured power system, *Energy Conversion and Management*, vol.45, no.15-16, pp.2297-2312, 2004.
[60] H. Bevrani, Y. Mitani and K. Tsuji, Sequential design of decentralized load frequency controllers using μ synthesis and analysis, *Energy Conversion and Management*, vol.45, no.6, pp.865-881, 2004.